

Franz-Keldysh and band-filling effects in the electroreflectance of highly doped *p*-type GaAs

J. M. A. Gilman and A. Hamnett

Department of Chemistry, Bedson Building, The University, Newcastle-Upon-Tyne NE1 7RU, England

R. A. Batchelor

Pilkington Technology Centre, Lathom, Ormskirk, Lancashire L40 5UF, England

(Received 8 April 1992; revised manuscript received 17 July 1992)

The electroreflectance of highly doped semiconductors has been modeled in terms of the Franz-Keldysh effect and the band-filling (Moss-Burstein) effect, including the spatial variation of the modulation. Calculations are compared to experimental electrolyte electroreflectance results obtained from $2 \times 10^{18} \text{ cm}^{-3}$ *p*-type GaAs electrodes in a dilute sulfuric-acid electrolyte. The form of the experimental line-shape variation with applied potential is successfully predicted, although it appears that only about a third of any change in dc potential applied to the electrode is actually dropped across the semiconductor space-charge region in samples of this dopant density. The relative significance of the Franz-Keldysh and Moss-Burstein effects is discussed in light of the possibility of band-gap narrowing.

INTRODUCTION

Electroreflectance^{1,2} (ER) and photorefectance^{3,4} have become popular as means to studying space-charge voltages and electric fields in semiconductors. Results are interpreted in terms of the Franz-Keldysh effect,^{5,6} using the theory developed by Aspnes,^{7,8} which describes the increasing width of the spectral line shape and higher energy oscillations as the electric field is increased. This analysis, when properly used, allows the determination of the dc field distribution in semiconductor depletion regions from experimental electroreflectance results, and has been applied to a variety of materials over the last twenty years.

For very low-doped samples, where the internal electric field is small the theory reduces under certain conditions to a simple third-derivative form,⁹ but it has recently been shown for moderate-to-highly doped semiconductors^{1,2} that the analysis of ER must take field inhomogeneity in the narrow depletion layer into account if accurate results are to be obtained. As a result of the field variation within the semiconductor the spectra take on features strongly dependent on the potential distribution, and it is these which give the technique much of its diagnostic value in elucidating the electric-field properties of the sample in question.

Electroreflectance has proved to be particularly useful as a means of determining space-charge voltages at the semiconductor-electrolyte interface. Analogy with the classical Schottky barrier would suggest that any change in the potential applied to a reverse-biased semiconductor electrode should be dropped across the semiconductors depletion region. In practice, depending on the electrolyte and applied potential used, it is possible that only a proportion of any change in applied potential will be dropped across the depletion layer, due to surface-state pinning of the Fermi level, and electroreflectance may then provide a valuable route to determining the degree of such pinning.

Despite the success which has been achieved in the modeling of spectra from moderately doped GaAs, we have found that results from more highly doped ($\geq 10^{18} \text{ cm}^{-3}$) samples cannot be so readily interpreted using Franz-Keldysh theory.² There are several reasons why difficulties might be encountered in understanding spectra from highly doped substrates, but in particular the effect of charge carriers occupying band minima and maxima and influencing optical absorption is likely to be important. This is known as the Moss-Burstein effect,^{10,11} and when doping is sufficiently high to bring Fermi level into the majority carrier band it leads to a shift of the absorption onset to higher energies. Cardona, Pollak, and Shaklee¹² observed the Moss-Burstein effect in GaAs electroreflectance, and it was subsequently studied in more detail in the electroreflectance of InSb by Glosser and co-workers^{13,14} as a means of distinguishing between critical points.

The effects of high carrier densities on the optical and electronic properties of GaAs have been the subject of considerable study over recent years, and in the present paper the implications of the Moss-Burstein effect for electroreflectance are considered and comparisons of calculations with experimental data are made. The magnitude of the band-filling effect will vary greatly with the potential within the space-charge layer, and the inclusion of this spatial variation will be essential if a quantitative treatment is to be developed. Spectra have been modeled for low reverse biases, and it has been necessary to use the Boltzmann approximation to model the potential distribution, as opposed to the simple Mott-Schottky depletion approximation.

THEORY

The theory underlying the optical properties of semiconductors has been well documented.¹⁵ The contribution of stimulated absorption to the imaginary part of the dielectric function $\epsilon = \epsilon_1 + i\epsilon_2$ at an M_0 critical point be-

tween two bands can be written as

$$\epsilon_2(\omega) = 8(\pi e/m\omega)^2 |\mathbf{a}_0 \cdot \mathbf{p}_{ij}|^2 J_{cv}, \quad (1)$$

where $|\mathbf{a}_0 \cdot \mathbf{p}_{ij}|$ is the corresponding matrix element, ω is the angular optical frequency, e and m are electronic charge and mass, respectively, and J_{cv} is the joint density of states. If parabolic bands are assumed close to the band gap and the matrix element is assumed to vary slowly, then above the band-gap energy $\hbar\omega_g (= E_g)$

$$\epsilon_2(\omega) = B_f(\omega - \omega_g)^{1/2}/\omega^2, \quad (2)$$

where B_f is a constant taking the interband matrix element and all other physical constants into account.

When an electric field \mathbf{E} is applied across the material, Aspnes showed that the dielectric function is distorted through the Franz-Keldysh effect by an additional amount,^{7,8}

$$\Delta_{fk} \epsilon_2(\omega) = (B_f |\Theta|^{1/2}/\omega^2) \text{Re}\{H(z)\}, \quad (3)$$

$$\Delta_{fk} \epsilon_1(\omega) = (B_f |\Theta|^{1/2}/\omega^2) \text{Im}\{H(z)\}, \quad (4)$$

where the real part of this distortion is obtained by a Kramers-Kronig transformation. Here, z is a complex number equal to $x + i\Gamma/\Theta$, where $x = (\omega_g - \omega)/\Theta$ and $\Theta = (E^2 e^2 / 2\mu\hbar)^{1/3}$, where $\hbar\Gamma$ is the collision broadening parameter and μ is the interband joint effective mass.

$H(z)$ is defined as

$$H(z) = \pi \{ Ai'^2(z) - z Ai^2(z) + i [Ai'(z) Bi'(z) - z Ai(z) Bi(z)] \} + iz^{1/2}, \quad (5)$$

the real and imaginary parts of which were calculated by means of numerical routines reported elsewhere.¹⁶ The prime superscript (') indicates differentiation with respect to the argument z .

In GaAs, transitions from both the light- and heavy-hole valence bands contribute to absorption, and by fitting Eq. (2) to experimental absorption spectra a combined value of B_f of $3.5 \times 10^{23} \text{ s}^{-3/2}$ can be obtained. Following our previous work in fitting GaAs electroreflectance,² we have taken a ratio of 1:2 for the ratio of light-hole to heavy-hole absorption, consistent with the findings of other researchers.^{3,17} In subsequent calculations the individual contributions of the light- and heavy-hole transitions to the Franz-Keldysh and Moss-Burstein effects have been calculated separately and then added together to give the total dielectric function modulation.

The presence of charge carriers in the conduction or valence bands decreases the density of states which can be excited by near-band-gap energy radiation and also leads to the possibility of stimulated emission occurring. These factors reduce ϵ_2 and for the simple two-band model the change in ϵ_2 due to band filling will be given by

$$\Delta_{mb} \epsilon_2(\omega) = B_f(\omega - \omega_g)^{1/2} \times [F_v(\omega) - F_c(\omega) - 1] u(\omega - \omega_g)/\omega^2, \quad (6)$$

where $u(x)$ is the unit step function. The subscript refers to the Moss-Burstein effect and $F_{v,c}(\omega)$ refer to the Fermi

occupation factors in the valence and conduction bands, respectively. In low-doped p -type semiconductor materials, these are usually very close to 1 and 0, corresponding to a full valence band and an empty conduction band. However, in a sample of sufficient doping the Fermi level will approach one of the band edges and change the occupation factors significantly.

The values of $F_v(\omega)$ and $F_c(\omega)$ are calculated for a large negative bias as shown in Fig. 1. The substrate Fermi level E_F is assumed to split in the depletion region into two quasi-Fermi levels, the majority quasi-Fermi level E_{Fp} staying approximately level, and the minority quasi-Fermi level E_{Fn} following the curvature of the valence- and conduction-band edges, in a similar manner to a solid-state p - n junction.¹⁸ This simple assumption is based on the nonconfinement of conduction-band electrons at the interface, and on the low rate of carrier generation/recombination for a wide-gap material such as GaAs at 300 K,¹⁹ and prevents miscalculation of minority occupation for biases beyond $-E_g/e$, which would occur using the assumption of a single constant Fermi level.

The occupation functions can now be written as

$$F_v(\omega) = 1/(1 + \exp\{[eV_s(y) - E_F + (E - E_g)\mu/m_{\text{eff}}]/kT\}), \quad (7)$$

$$F_c(\omega) = 1/(1 + \exp\{[(E - E_g)(\mu/m_{\text{eff}} - 1) - E_F - E_g]/kT\}), \quad (8)$$

where $V_s(y) = |V(y) - V_{(\text{subs})}|$ is the absolute value of the electric potential step at distance y into the substrate from the substrate potential $V_{(\text{subs})}$ (here equal to the substrate valence-band potential E_v) due to space-charge depletion, m_{eff} is the effective mass in the majority band, and E_F is defined for the bulk as positive inside the majority band, negative in the band gap. Similar expressions were obtained by Lukes and Humlicek,²⁰ although these appear to contain small algebraic errors, specifically use

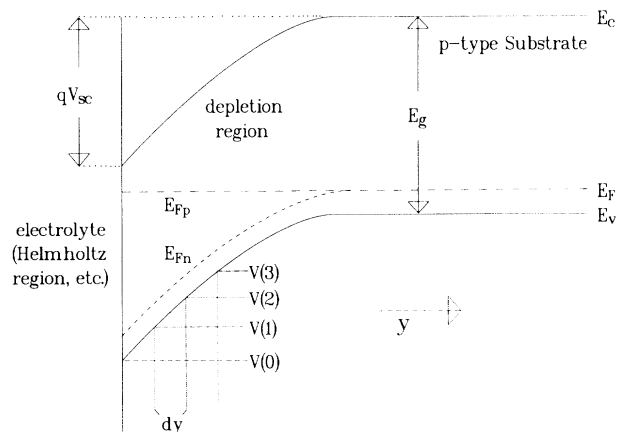


FIG. 1. Band-edge profile of reverse-biased GaAs-electrolyte interface. The majority quasi-Fermi level (E_{Fp}) stays constant in the semiconductor, while the minority quasi-Fermi level (E_{Fn}) follows the band-edge curvature.

of a term $[\mu/(2m_v)]$ in Eqs. (6) and (7) in their paper, where the use of (μ/m_v) would have been correct.

The change $\Delta_{mb}\epsilon_2(\omega)$ will be associated with a corresponding change in the real part of the dielectric function, which can be calculated by a Kramers-Kronig transformation

$$\Delta_{mb}\epsilon_1(\omega) = (2/\pi)\mathcal{P} \int_0^\infty \omega' \Delta_{mb}\epsilon_2(\omega') d\omega' / [(\omega')^2 - \omega^2], \quad (9)$$

where \mathcal{P} denotes the principal value of the integral.

The above theory has been well documented elsewhere,^{20,21} but in order to calculate the electroreflectance spectra quantitatively the distribution of electric field and potential near the semiconductor surface must be considered.²² For a semiconductor electrode held at reverse bias, the carrier density near the surface will be very low, while the electric field will be large. As a result, the Franz-Keldysh effect will tend not to be strongly influenced by band filling, because the contribution of the Franz-Keldysh effect to the electroreflectance will arise predominantly from regions near the surface, where the field modulation is large. On moving into the semiconductor the carrier concentration will increase, and near the back of the depletion layer the Moss-Burstein effect will increase rapidly. If spectra are measured with a small ac modulation superimposed on a dc reverse bias, then the depletion layer width will oscillate slightly and the ac Moss-Burstein optical modulation will be concentrated at the back of the depletion layer, in a similar manner to the modulation observed in exciton electroreflectance.²³ The sensitivity of the Moss-Burstein effect to small variations in potential at the back of the depletion layer makes it important to model the potential distribution carefully, and our approach is described in the next section.

COMPUTATIONAL METHOD

The interface was modeled numerically for light impinging on, and being reflected from, the GaAs surface in aqueous electrolytes. A finite-difference scheme was used to model the band-edge profile (see Fig. 1). The potential at the interface was fixed at the space-charge potential V_{sc} , and the variation of the potential V along y was calculated using the equations

$$d^2V/dy^2 = -\rho/\epsilon_s = (V_{(i+1)} - 2V_{(i)} + V_{(i-1)})/(dy)^2, \quad (10)$$

where the first part of (10) refers to Poisson's equation (where ρ is charge density and ϵ_s is the electrostatic dielectric constant), and the second is the three-point finite-difference approximation to the second derivative of V . Each successive point is calculated by manipulating (10), to give

$$V_{(i+1)} = 2V_{(i)} - V_{(i-1)} - (\rho/\epsilon_s)(dy)^2. \quad (11)$$

The value of ρ was taken using the Boltzmann approximation, which can be shown to be

$$\rho = eN_a (1 - \exp\{-e[|V_{(i)} - V_{(subs)}|]/kT\}) \quad (12)$$

for acceptor density N_a and Boltzmann thermal energy kT . The correct profile was found by trial-and-error iteration of the second potential point, such that the potential close to the substrate approached the correct value, along with a zero-field substrate condition. Some 120 discrete films were used over a distance of $10\lambda_{db} + W_{dep}$, where the former term is 10 times the Debye length $[\lambda_{db} = (\epsilon_s kT/N_a)^{1/2}/e]$ and is the characteristic exponential decay length for potential variations in semiconductors¹⁹, and the latter is the depletion-layer width for a given space-charge potential V_{sc} . The addition of the former allowed the Moss-Burstein effect to be accurately calculated, and comparisons were made with the simpler depletion-layer approximation, the results of which confirmed the necessity of the extra width for correct modeling of this phenomenon.

The reflectivity was calculated using an implicit multifilm light reflection routine as was reported earlier, taking the dielectric properties at each point to be the sum of the zero-field properties and the distortions due to the Franz-Keldysh and Moss-Burstein effects. It should be noted that no cross term between the latter two effects was required, due to the former principally resulting from the high fields near the surface, where depletion of carriers is most efficient, while the latter arises mainly close to the substrate, where the bands are nearly flat. An energy scale of 180 points between 1.2–2.6 eV was taken, allowing for accurate integrating of the Kramers-Kronig expressions. The reflection spectra for two values of V_{sc} differing by V_{os} (the effective oscillatory term in the space-charge region) were subtracted, to give the value of $\Delta R/R$. The technique has been described previously in greater detail.² The collision broadening parameter for the $E_0 (=E_g)$ light- and heavy-hole transitions was taken as $\hbar\Gamma_0 = 12$ meV, while that for the $E_0 + \Delta_0$ spin-orbit split-off transition used $\hbar\Gamma_0 = 15$ meV, similar to values used for lower doped samples.

In common with our earlier work, the Franz-Keldysh collision broadening is allowed to increase exponentially with energy above the band gap, with $\Gamma = \Gamma_0 \exp[\delta(\omega - \omega_g)]$ and $\delta = 4$ eV⁻¹ for this sample. This is to account for the increasing rapidity of collision-assisted electron-hole recombinations at higher energy separations (and hence greater carrier velocities). The Moss-Burstein modulation is comparatively broad and featureless, so no further broadening was applied to it, because broadening produces no significant improvement in the fit to experimental data. The value of the spin-orbit split-off energy $E_g + \Delta_0$ was taken to be 1.765 eV, while the value of E_g was 1.405 eV, about 20 meV smaller than the normal literature values²⁴ for 300 K. A similar shift has been observed in other GaAs electrodes,²⁵ and may be related to the phenomenon of band-gap narrowing,²⁶ which is discussed later in this paper.

EXPERIMENTAL METHOD

Results were obtained from electrolyte electroreflectance (EER) experiments at 300 K on the exposed

$\langle 100 \rangle$ face of an electrode from a Zn-doped GaAs wafer with a donor density estimated (by Hall effect) at $2 \times 10^{18} \text{ cm}^{-3}$. A 0.5-M H_2SO_4 electrolyte ($pH=0$) was used and applied potentials were measured with respect to a $\text{Hg}/\text{Hg}_2\text{SO}_4$ reference electrode. A 15-mV sinusoidal modulation was superimposed on dc biases of between -0.5 and -1.2 V, and phase-sensitive detection was used to examine the reflectance of s -polarized light. The ac signal frequency used for the results included here was 440 Hz, and no frequency dependence was observed for spectra taken at other frequencies between 40 and 1000 Hz. The sinusoidal wave form avoids the problems associated with higher harmonics found in other wave forms (e.g., square, sawtooth, etc.). The use of a small modulation of a larger applied voltage permits analysis of the potential and field profiles, along with surface processes, at the dc bias in question, since the small size of the modulation used here enables us to assume a linear relationship between ac and spectrum amplitudes.² This would be less easily facilitated with results taken over a larger voltage range (e.g., between the applied voltage in question and a reference at flatband), as the significant features of the spectrum become smoothed out, hindering interpretation.

Further details are included in an earlier paper,² in which it was reported that this sample, unlike similar samples of lower dopant density, resisted all attempts at accurate modeling if the assumption was made that the 15-mV applied oscillatory voltage V_{mod} was entirely accommodated across the semiconductor depletion layer. Results for applied voltages of $V_{\text{appl}} = -0.5$, -0.9 , and -1.2 V versus $\text{Hg}/\text{Hg}_2\text{SO}_4$ are given in Fig. 2, and the best available theoretical fits corresponding to these data sets are given in Fig. 3. Both the experimental and theoretical plots show the normalized reflectance modulation for modulation toward decreasing reverse bias. When Figs. 2 and 3 are compared, the main features of the calculated spectra can be seen to follow those observed experimentally, and this is described in greater detail below.

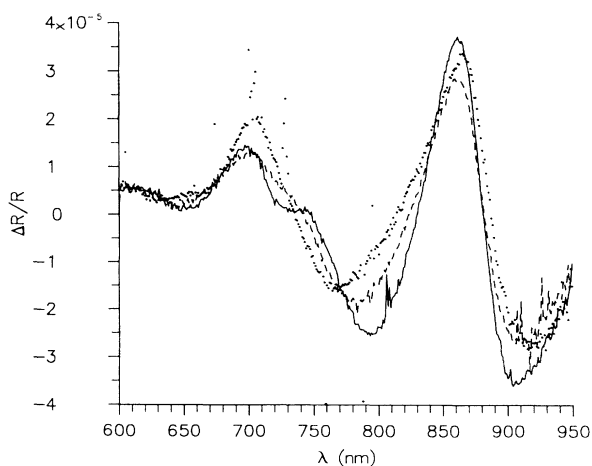


FIG. 2. EER results for a 2×10^{18} p -type GaAs sample. The applied potential V_{appl} varies between -0.5 , -0.9 , and -1.2 V vs $\text{Hg}/\text{Hg}_2\text{SO}_4$, for full, dashed, and dotted lines, respectively.

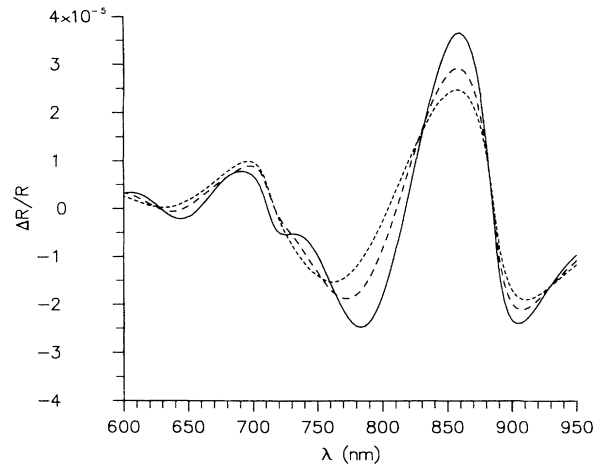


FIG. 3. Best available theoretical fits to compare with Fig. 2. V_{sc} varies between 0.28, 0.39, and 0.52 V, for full, long-dashed, and short-dashed lines respectively, and oscillatory potentials of $V_{\text{os}} = 5$, 5.25, and 5.75 mV, respectively, give the closest fits.

The Hall-effect-measured dopant density of $2 \times 10^{18} \text{ cm}^{-3}$ was confirmed by capacitance voltage measurements obtained at 10 kHz by sweeping the reverse bias to increasing values. At lower modulation frequencies substantial frequency dispersion of the electrode capacitance was observed, and the measured capacitance rose quite rapidly as the frequency dropped below 2000 Hz.

DISCUSSION

Theoretical spectra were fitted to experiment and the best fit to the result at -0.5 V versus $\text{Hg}/\text{Hg}_2\text{SO}_4$ was obtained by using a space-charge voltage of $V_{\text{sc}} = 0.28$ V, Fig. 4. As can be seen, the calculated spectrum combining both the Franz-Keldysh and the band-filling effects follows the main features of the experimental results faithfully. However, in order to match the spectrum sizes, it has been necessary to assume that a modulation of only $V_{\text{os}} = 5.75$ mV is dropped across the space-charge layer, rather than the 15-mV modulation which was applied to the electrode. The calculations for the Franz-Keldysh effect alone and for the Moss-Burstein effect alone are also given and the inclusion of the latter improves the ratio of the peak height at 860 nm to the valley depth at 785 nm. The individual contributions add approximately linearly to give the combined result for the two effects.

It has prove difficult to match the exact position of features at lower wavelengths, which appear slightly displaced vertically from the experimental results, and there also appear to be slight discrepancies between the observed and calculated valley depths at wavelengths above 900 nm. The width of the main peak around 800–900 nm, together with the horizontal displacement of the trough feature near 775 nm, may be due to nonparabolicity effects, concerning which we have performed preliminary calculations based on available theory and data,^{27,28} and which appear to give results consistent with the observed shift.

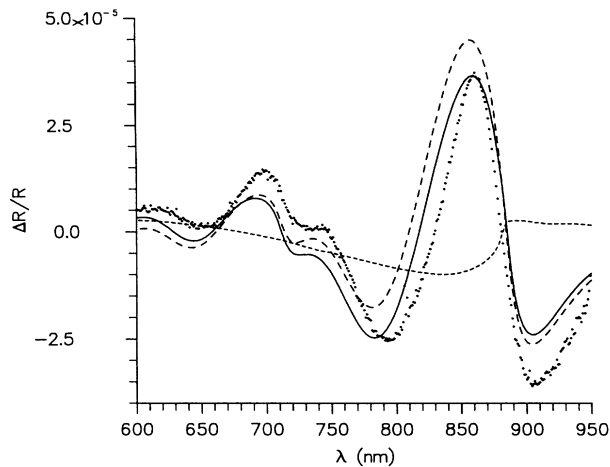


FIG. 4. Comparison between calculated (full line), and experimental (dotted line) results, including the individual Franz-Keldysh (long-dashed line) and Moss-Burstein (short-dashed line) contributions. The applied voltage V_{appl} is -0.5 V vs Hg/Hg₂SO₄ and the semiconductor space-charge potential V_{sc} is 0.28 V.

The best fit to the -0.9 -V versus Hg/Hg₂SO₄ result is given in Fig. 5. When comparisons are made with Fig. 2–4, it can be seen that the motion of the Franz-Keldysh oscillation at 740 nm in Fig. 4 to higher energies with increasing reverse bias and its eventual merging into the spin-orbit split feature at 680 nm are clearly followed in the calculated results. Similarly, the movement of the peak near 850 nm and the valley near 780 nm are modeled. Again, the separate contributions for the Franz-Keldysh and Moss-Burstein effects are shown, as they are for $V_{\text{appl}} = -1.2$ V versus Hg/Hg₂SO₄ in Fig. 6. At the latter applied potential it becomes significantly more difficult to model accurately the shape of low-

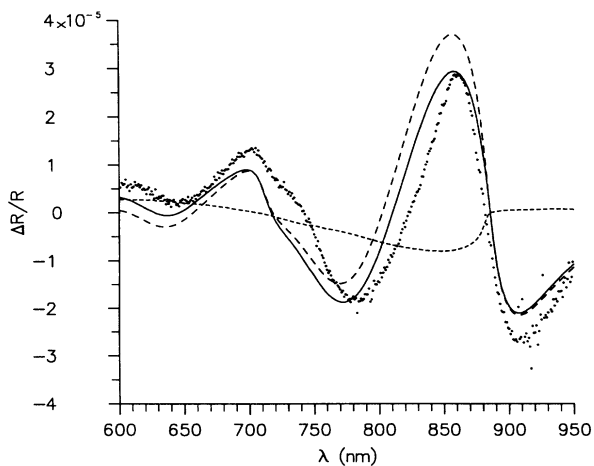


FIG. 5. Comparison between calculated (full line), and experimental (dotted line) results, including the individual Franz-Keldysh (long-dashed line) and Moss-Burstein (short-dashed line) contributions. The applied voltage V_{appl} is -0.9 V vs Hg/Hg₂SO₄ and the semiconductor space-charge potential V_{sc} is 0.39 V.

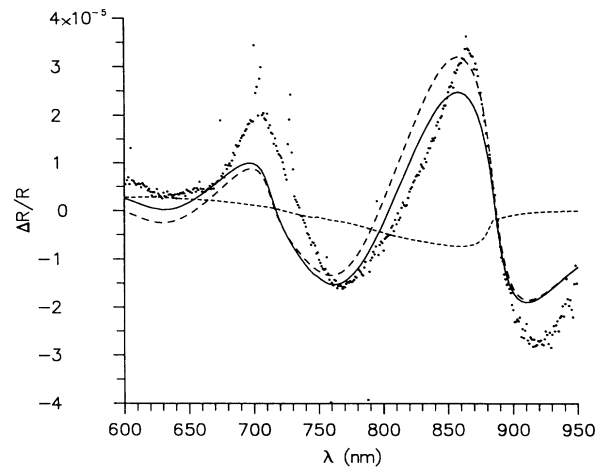


FIG. 6. Comparison between calculated (full line), and experimental (dotted line) results, including the individual Franz-Keldysh (long-dashed line) and Moss-Burstein (short-dashed line) contributions. The applied voltage V_{appl} is -1.2 V vs Hg/Hg₂SO₄ and the semiconductor space-charge potential V_{sc} is 0.52 V.

wavelength features, and the experimental peak near 875 nm is observed to take a value higher than that for the -0.9 -V value of V_{appl} , in contrast with the observed and calculated decrease of the corresponding peak for lower applied potentials. A number of comments may be made concerning these results.

First, to fit to these curves, several assumptions were necessary. Although the experimental modulation voltage V_{mod} was 15 mV, the modeled values of V_{os} were 5.75 , 5.25 , and 5.00 mV for the $V_{\text{appl}} = -0.5$, -0.9 , and -1.2 V versus Hg/Hg₂SO₄ cases, respectively. The optimal theoretical space-charge voltages for the three sets of results were $V_{\text{sc}} = 0.28$, 0.39 , and 0.52 V, respectively, although the accuracy of the last is debatable owing to the failure of the modeled spectra to follow closely the experimental features at the lower wavelengths. Hence, an increase in reverse bias for the electrode of 0.7 V appears to correspond to a change in the semiconductor space-charge voltage of just 0.24 V, suggesting that about 65% of any change in applied voltage is accommodated outside the depletion layer. This degree of Fermi-level pinning is larger than that deduced in our earlier interpretation² because of the use of a measured dopant density in the present calculations, instead of our previous use of a lower dopant density in order to facilitate fitting.

Similarly, only about 35% of the modulation voltage seems to be accommodated within the space-charge layer. Thus only about 35% of any ac modulation and 35% of any change in applied dc potential appears to be dropped across the space-charge layer for the results reported here. In contrast, previous work on less highly doped samples^{2,25} was able to predict the magnitude of electroreflectance spectra by assuming that all the applied ac modulation was dropped across the space-charge layer. The anomalous behavior of 2×10^{18} cm⁻³-doped samples correlates with their nonideal capacitance voltage response, which shows a considerable increase in inter-

face capacitance for modulations of frequencies below 2 kHz. The increase in capacitance indicates the presence of rapid surface processes, such as surface-state charging, which may contribute to part of the applied potential oscillation being dropped at the electrode surface, rather than across the depletion layer. The electrode impedance can be observed to drift over a time scale of minutes, while some variability in electroreflectance spectra taken at identical applied potentials was also noted. The changes which occur at the surface of a *p*-type GaAs electrode in dilute sulfuric acid with applied potential are therefore of some complexity and it is interesting to note that a similar degree of Fermi-level pinning appears to operate for both 440-Hz ac and dc applied potential changes.

Fermi-level pinning effects of this magnitude were not commonly seen on samples of lower dopant density, and results coincide with the decreasing electrochemical stability of more highly doped samples. This is likely to be connected to the decreasing widths of and larger electric fields in the space-charge regions of more highly doped samples, which will allow the more rapid communication of charge carriers between surface states and the bulk. Transfer would be further enhanced in the presence of intragap hopping states within the space-charge layer. It may be worth noting that the dopant density is approaching the approximate level required to permit interband tunneling processes (i.e., $\sim 3 \times 10^{18} \text{ cm}^{-3}$ for efficient Esaki diode operation).²⁹ In the case of tunneling to an intragap surface state rather smaller voltages should be needed, because of the smaller energy gap between the surface state and the band edge. For more highly doped semiconductor electrodes, changes in applied potential are therefore likely to lead to the transfer of carriers across the depletion layer, which will allow changes in surface-state population or surface chemistry and hence significant Fermi-level pinning. In common with electrodes of lower dopant density, such effects will be sensitive to electrode etching and pretreatment procedures.

The fitting of theory to experiment was performed by varying each parameter over a decreasing range, until best fits for each spectrum were found. The evolution of spectral features around a smaller voltage range (0.23–0.33 V) is illustrated in Fig. 7 for the $V_{\text{appl}} = -0.5$ V case, and it is clear that the motion of the relative positions of the peaks and troughs in the longer wavelength range, along with that of the Franz-Keldysh oscillation around 740 nm, can be followed and the space-charge voltage estimated by fitting. A similar process was used to estimate the position of the Fermi level, as is shown in Fig. 8 for the spectrum taken for $V_{\text{appl}} = -0.9$ V. The line shapes calculated for bulk Fermi levels 55, 75, and 95 meV into the band gap are shown, and the iteration process may again be seen to give a best fit for $E_F = E_V + 75$ meV.

The position of the bulk Fermi level is of great importance in determining the strength of the modulation resulting from band filling. A simple calculation based on the assumption of parabolic bands suggests that $E_F = E_V + 24$ meV for $N_a = 2 \times 10^{18} \text{ cm}^{-3}$, and the inclusion of band nonparabolicity leads to $E_F = E_V + 39$

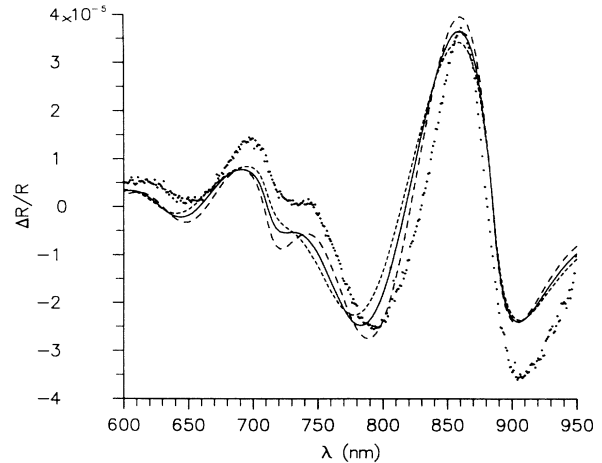


FIG. 7. Evolution of the calculated spectra with space-charge voltage, compared with experimental results at $V_{\text{appl}} = -0.5$ V vs Hg/Hg₂SO₄. $V_{\text{sc}} = 0.23, 0.28,$ and 0.33 V (long-dashed, full, and short-dashed lines, respectively).

meV.²⁴ Theoretical spectra obtained using different bulk Fermi levels for the calculation of the band-filling modulation, one example of which was given in Fig. 8, have shown that the expected bulk majority-carrier Fermi level leads us to considerably overestimate the influence of band filling on the spectra. Instead, the slightly arbitrary use of $E_F = E_V + 75$ meV gives more satisfactory agreement with experimental spectra and implies that the Moss-Burstein effect in *p*-type GaAs electroreflectance spectra is smaller than would be expected.

Band filling has been found to shift the absorption onset in *n*-type GaAs to higher energy, but the shift is usually less than would be expected on the basis of the theory we have presented and *p*-type doping shifts the absorption edge to lower energies.³⁰ The apparent shrinkage of the band gap, which is responsible for this effect, can be attributed to dopant-induced band tailing^{26,31} and

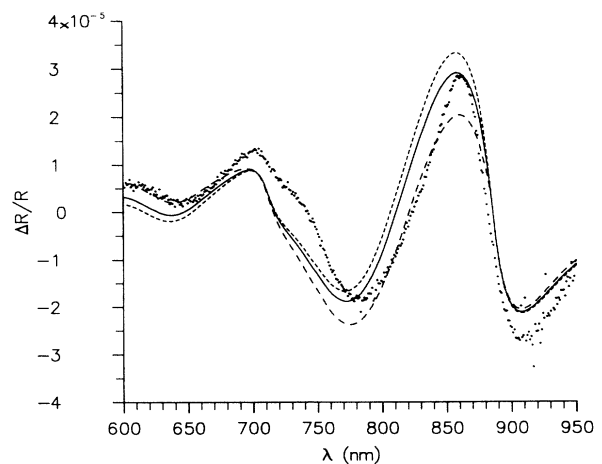


FIG. 8. Variation of the calculated spectra with the Fermi-level position for $V_{\text{appl}} = -0.9$ V vs Hg/Hg₂SO₄ and $V_{\text{sc}} = 0.39$ V. $E_F = 55, 75,$ and 95 meV into the band gap (for long-dashed, full, and short-dashed lines, respectively).

to many-body interactions such as exchange and correlation effects.³² The band-gap shrinkage tends to compensate the Moss-Burstein effect and it is therefore unsurprising that the approach presented above will tend to overestimate the influence of band filling on electroreflectance spectra. While an estimate can be made of the degree of band-gap shrinkage, any useful inclusion of the effect into the calculation of electroreflectance would require us to be able to calculate the modulation of the absorption over a wide wavelength range, in order to obtain the changes in both the real and imaginary parts of the dielectric function. Furthermore, previous theoretical work has concentrated on the differences between the optical properties of doped and undoped semiconductors, whereas electroreflectance involves the changing of majority-carrier density in the presence of a constant dopant atom concentration. The formulation of a practical approach to this problem therefore involves some difficulty, and for the work presented here we have used the empirical method of choosing a value for E_F to fit experimental data.

POSSIBLE SOURCES OF DISCREPANCIES BETWEEN THEORY AND EXPERIMENT

Two more points must be taken into consideration as possible explanations for the unaccountable but consistent differences between the theoretical and observed spectra (such as poor fitting at lower wavelengths and the anomalously low valley depth at higher wavelengths). First, excitonic transitions³³ could conceivably be responsible for features just beneath the energy gap E_g , such as the valley discrepancy around 910–940 nm in Figs. 2–4. However, the relatively high fields in a sample as highly doped as this (with $E_{av}/E_I \sim 50$, where E_{av} is the average electric field over the depletion region and E_I is the ionization field³³), combined with temperatures corresponding to thermal energies much higher than the binding (and, hence, ionization) energy of the exciton ($kT \sim 25$ meV, $R \sim 5$ meV, where R is the effective exciton Rydberg energy³³), suggest that the broadening of any excitonic absorption will be so great as to render the effect unobservable given the size of the other contributions.

As for excitonic transitions in the low-field depletion-layer-substrate interface region, the high temperature, combined with the fact that most of the potential (and therefore field) modulation within the semiconductor is accommodated in the depletion region close to the interface, would still seem to imply that any excitonic signal would be minimal in effect. In our earlier results for lower-doped samples,² the observed spectra could be accurately described without invoking the excitonic effect, despite the greater probability of observing such transitions due to lower field in such samples. More recently, it has been possible to model n -type GaAs samples of doping density $\sim 1 \times 10^{18} \text{ cm}^{-3}$,³⁴ again neglecting excitons, with a much higher degree of accuracy than in the case given here. Because the electric field will be higher in the $2 \times 10^{18} \text{ cm}^{-3}$ case, it would therefore seem that such effects are unlikely to be responsible for the deviations between theory and experiment, and it is by no means clear

if differences in doping polarity, or even sample quality, may account for the comparative ease of fitting for n -type samples.

Another mechanism which may distort EER spectra is that of the change in the matrix element due to the extreme inhomogeneity of the electric field, which drops from a maximum at the interface to a decaying form within the substrate within a distance much smaller than that corresponding to an optical decay length. The assumption we have used of a localized Airy function form for field-dependent absorption requires reassessment, particularly for energies much higher than the band gap, although the better fits achievable with n -type samples of only slightly lower dopant density³⁴ suggest this not to be a major factor, as the matrix elements should not change so rapidly over such a small range of doping density (and, hence, electric field). When we compare with Del Sole and Aspnes³⁵ condition for negligible effects from nonuniformity of field, which can be written (in our form of notation) as

$$\hbar \Theta |dE/dy| (eE^2)^{-1} \ll 1, \quad (13)$$

we find the left-hand term to be about 0.16 for typical values of field and space-charge potential. It is likely that this effect will require proper treatment at much higher dopant densities, but the above result suggests we may be confident with the results for the case in question here.

CONCLUSIONS

Electrolyte electroreflectance from $2 \times 10^{18} \text{ cm}^{-3}$ p -type GaAs was modeled in terms of the Franz-Keldysh and the Moss-Burstein effects. Accuracy was increased by using a Boltzmann approximation rather than a simple depletion-layer model to calculate the potential and carrier distributions near the surface of a semiconductor electrode held in depletion. The results of the models appear to follow the experimentally observed features with reasonable accuracy, although several problems remain to be fully resolved.

Band filling is found to be less important in determining the spectral line shape than would be predicted from a simple Moss-Burstein calculation, and the deviation was attributed to the effects responsible for band-gap narrowing. Direct comparison of the changes in optical properties with dopant density are, however, only likely to provide qualitatively insight into this problem, because in electroreflectance it is the optical response from the modulation of carrier density in the presence of *constant* dopant atom concentration which is of interest. The doping-induced changes in the optical properties of the semiconductor under zero modulation will have very little influence on the electroreflectance spectra.

The electroreflectance spectral line shape was observed to change more slowly with the applied potential than predicted, and the spectrum amplitudes were smaller than predicted, despite the fact that both these characteristics are successfully modeled in samples of lower dopant density. The quite considerable deviation of the $2 \times 10^{18} \text{ cm}^{-3}$ p -type GaAs electroreflectance from an otherwise successful model suggests that only about 35%

of any change in dc or 440-Hz ac applied potential is dropped across the semiconductor space-charge layer, because of partial Fermi-level pinning by surface states. While the possibility remains of a breakdown of the Franz-Keldysh theory at this dopant density, our interpretation is supported by the nonideal electrochemistry of the present samples and their rapid increase in interface capacitance below 2 kHz. More detailed study of the influence of surface states on Fermi-level pinning pro-

cesses should therefore be possible by studying electroreflectance over a wide range of modulation frequencies.

ACKNOWLEDGMENTS

This work was supported by the Science and Engineering Research Council (U.K.). We are grateful to A. C. Brown for the experimental work discussed here.

-
- ¹U. Behn and H. Röppischer, *J. Phys. C* **21**, 5507 (1988).
²R. A. Batchelor, A. C. Brown, and A. Hammett, *Phys. Rev. B* **41**, 1401 (1990).
³C. Van Hoof, K. Deneffe, J. DeBoeck, D. J. Arent, and G. Borghs, *Appl. Phys. Lett.* **54**, 608 (1989).
⁴O. K. Gaskill, N. Bottka, and R. S. Sillman, *J. Vac. Sci. Technol. B* **6**, 1497 (1988).
⁵W. Franz, *Z. Naturforsch* **13**, 484 (1958).
⁶L. V. Keldysh, *Zh. Eksp. Teor. Fiz.* **34**, 1138 (1958) [*Sov. Phys. JETP* **7**, 788 (1958)].
⁷D. E. Aspnes, *Phys. Rev.* **147**, 554 (1966).
⁸D. E. Aspnes, *Phys. Rev.* **153**, 973 (1967).
⁹D. E. Aspnes, *Surf. Sci.* **37**, 418 (1973).
¹⁰T. S. Moss, *Proc. Phys. Soc. London Sect. B* **76**, 775 (1954).
¹¹E. Burstein, *Phys. Rev.* **93**, 632 (1954).
¹²M. Cardona, F. H. Pollak, and K. L. Shaklee, in *Proceedings of the International Conference on the Physics of Semiconductors, Kyoto, 1966* [*J. Phys. Soc. Jpn. Suppl.* **21**, 89 (1966)].
¹³R. Glosser and B. O. Seraphin, *Phys. Rev.* **187**, 1021 (1969).
¹⁴R. Glosser, J. E. Fischer and B. O. Seraphin, *Phys. Rev. B* **1**, 1607 (1970).
¹⁵F. Wooten, *Optical Properties of Solids* (Academic, New York, 1972).
¹⁶A. Hamnett, J. M. A. Gilman, and R. A. Batchelor, *Electrochim. Acta* **37**, 949 (1992).
¹⁷D. E. Aspnes, *Phys. Rev. B* **12**, 2297 (1975).
¹⁸H. K. Gummel, *IEEE Trans. Electron. Devices* **11**, 455 (1964).
¹⁹S. M. Sze, *Physics of Semiconductor Devices*, 2nd ed. (Wiley, New York, 1981).
²⁰F. Lukeš and J. Humlíček, *Phys. Rev. B* **6**, 521 (1972).
²¹N. Döhler and G. H. Döhler, *Superlatt. Microstruct.* **6**, 357 (1989).
²²J. D. Axe and R. Hammer, *Phys. Rev.* **162**, 700 (1967).
²³F. Evangelisti, A. Frova, and S. U. Fischbach, *Surf. Sci.* **37**, 841 (1973).
²⁴J. S. Blakemore, *J. Appl. Phys.* **53**, R123 (1982).
²⁵R. A. Batchelor, A. Hamnett, R. Peat, and L. M. Peter, *J. Appl. Phys.* **70**, 266 (1991).
²⁶R. A. Abrams, G. J. Rees, and B. H. Wilson, *Adv. Phys.* **27**, 799 (1978).
²⁷G. M. Wysin, D. L. Smith, and A. Redondo, *Phys. Rev. B* **38**, 12 514 (1988).
²⁸D. E. Aspnes, *Phys. Rev. B* **10**, 4228 (1974).
²⁹U. Prechtel, Ch. Zeller, G. Abstreiter, and K. Ploog, in *International Symposium on GaAs and Related Compounds, Biarritz, 1984*, edited by B. de Cremoux, IOP Conf. Proc. No. 74 (Institute of Physics and Physical Society, London, 1985), Chap. 5, p. 339.
³⁰H. C. Casey, D. D. Sell, and K. W. Wecht, *J. Appl. Phys.* **46**, 250 (1975).
³¹H. C. Casey and F. Stern, *J. Appl. Phys.* **47**, 631 (1976).
³²H. S. Bennett and J. R. Lowney, *J. Appl. Phys.* **62**, 521 (1987).
³³D. F. Blosssey, *Phys. Rev. B* **2**, 3976 (1970).
³⁴J. M. A. Gilman, R. Hutton, R. Hamnett, and L. M. Peter (unpublished); J. M. A. Gilman, A. Hamnett, and R. A. Batchelor (unpublished).
³⁵R. Del Sole and D. E. Aspnes, *Phys. Rev. B* **17**, 3310 (1978).